УДК 551.465.62

© *А. А. Коник*[1,2*], *А. В. Зимин*[1,2], *И. Е. Козлов*[3], 2021
© Перевод: *К. А. Круглова*, 2021
[1]Институт океанологии им. П.П. Ширшова РАН, 117997, Нахимовский пр., д. 36, г. Москва, Россия
[2]Санкт-Петербургский государственный университет, 199034, Университетская наб., 7–9, г. Санкт-Петербург, Россия
[3]Морской гидрофизический институт РАН, 299011, Капитанская ул., 2, г. Севастополь, Россия
*E-mail: konikrshu@gmail.com

ПРОСТРАНСТВЕННО-ВРЕМЕННАЯ ИЗМЕНЧИВОСТЬ ХАРАКТЕРИСТИК ПОЛЯРНОЙ ФРОНТАЛЬНОЙ ЗОНЫ В БАРЕНЦЕВОМ МОРЕ В ПЕРВЫЕ ДВА ДЕСЯТИЛЕТИЯ XXI ВЕКА

Поступила в редакцию 07.06.2021, после доработки 05.10.2021

Рассматривается пространственно-временная изменчивость характеристик Полярной фронтальной зоны (ПФЗ) в Баренцевом море в поверхностном слое за теплые сезоны с 2002 по 2020 гг. Кроме этого, проводится анализ повторяемости малых вихревых структур в области фронтальной зоны в разные годы и описывается связь характеристик ПФЗ с глобальными атмосферными процессами. Положение и характеристики ПФЗ в поверхностном слое Баренцева моря определялись на основе кластерного анализа, выделялись по данным спутниковых измерений. Вихревые структуры в области ПФЗ детектировались по изображениям радиолокаторов с синтезированной апертурой (РСА) Envisat Asar и Sentinel-1A/B. Для оценки влияния атмосферных процессов на характеристики ПФЗ использовались индексы NAO, EA, EA/WR и SCAND. Установлено, что внутригодовые значения горизонтальных градиентов температуры и солености в области ПФЗ оставались стабильными в течение теплого сезона и составляли 0.05 °С/км и 0.02 ‰/км, соответственно. Изменчивость межгодовых характеристик градиента температуры ПФЗ составила от 0.02 °С/км до 0.08 °С/км, солености от 0.01 до 0.03 ‰/км, площади — от 120 до 425 тыс. км^2. Установлено, что максимальные среднемесячные значения площади ПФЗ отмечались в 2007 г., а минимальные — в 2003 г. Полученные результаты показали, что после 2010 г. величина горизонтальных градиентов температуры и солености ПФЗ в поверхностном слое уменьшилась, что, вероятно, связано с процессом «атлантификации» Баренцева моря. Максимальное количество малых вихревых структур в области ПФЗ отмечалось в 2009 г. Показано, что индекс SCAND за предшествующий зимний сезон можно использовать в качестве предиктора для прогноза характеристик ПФЗ в летний период.

Ключевые слова: температура поверхности моря, соленость поверхности моря, спутниковые наблюдения, кластерный анализ, Полярная фронтальная зона, малые вихри, NAO, EA, EA/WR, SCAND, Баренцево море.

© *A. A. Konik*[1,2*], *A. V. Zimin*[1,2], *I. E. Kozlov*[3], 2021
© Translation: *K. A. Kruglova*, 2021
[1]Shirshov Institute of Oceanology, Russian Academy of Sciences, 117997, Nahimovskiy prospekt, 36, Moscow, Russia
[2]St. Petersburg State University, 199034, 7–9, Universitetskaya Nab., St. Petersburg, Russia
[3]Marine Hydrophysical Institute, Russian Academy of Sciences, 299011, Kapitanskaya Str., 2, Sevastopol, Russia
*E-mail: konikrshu@gmail.com

SPATIAL AND TEMPORAL VARIABILITY OF THE POLAR FRONTAL ZONE CHARACTERISTICS IN THE BARENTS SEA IN THE FIRST TWO DECADES OF THE XXI CENTURY

Received 07.06.2021, in final form 05.10.2021

The article considers the spatial and temporal variability of the Polar Frontal Zone (PFZ) characteristics in the Barents Sea during the warm season from 2002 to 2020. In addition, the occurrence of small eddy structures in the PFZ region in different years is investigated, and the relationship of the characteristics of the frontal zone with global atmospheric processes is described. The position and characteristics of the PFZ were derived from satellite measurements using the cluster analysis method. Eddy structures in the PFZ region were detected from images of Envisat Asar and Sentinel-1A/B synthetic aperture radars. The NAO,

Ссылка для цитирования: *Коник А.А.*, *Зимин А.В.*, *Козлов И.Е.* Пространственно-временная изменчивость характеристик полярной фронтальной зоны в Баренцевом море в первые два десятилетия XXI века // Фундаментальная и прикладная гидрофизика. 2021. Т. 14, № 4. С. 39–51. doi: 10.7868/S2073667321040043

For citation: *Konik A.A.*, *Zimin A.V.*, *Kozlov I.E.* Spatial and Temporal Variability of the Polar Frontal Zone Characteristics in the Barents Sea in the First Two Decades of the XXI Century. *Fundamentalnaya i Prikladnaya Gidrofizika*. 2021, 14, 4, 39–51. doi: 10.7868/S2073667321040043

EA, EA/WR and SCAND indices were used to assess the influence of atmospheric processes on the PFZ properties. It was found that the intra-annual values of temperature and salinity gradients in the PFZ region remained stable during the warm season and reached 0.05 °C/km and 0.02 %/km, respectively. The variability of the interannual estimates of the PFZ properties ranged from 0.02 °C/km to 0.08 °C/km in temperature, from 0.01 to 0.03 %/km in salinity, and from 120,000 to 425,000 km^2 in area. The maximum monthly mean values of the PFZ area were observed in 2007, while the minimum — in 2003. The obtained results clearly showed that the intensity of the PFZ decreased after 2010, which is presumably related to the "Atlantification" of the Barents Sea. The maximum number of small eddy structures in the PFZ region was identified in 2009. It is shown that the SCAND index for the previous winter season can be used as a predictor for predicting the characteristics of the PFZ in the summer period.

Key words: sea surface temperature, sea surface salinity, satellite observations, cluster analysis, Polar frontal zone, small eddies, NAO, EA, EA/WR, SCAND, Barents Sea.

1. Introduction

In recent decades, significant changes have been observed in the Arctic region [1], which are reflected in the decrease in the area of the ice cover [2] and the "Atlantification" of polar waters [3]. This variability also affects the position of the frontal zones, the meandering of the frontal sections and the formation of eddy structures [4, 5].

Frontal zones and eddy structures in the World Ocean are an important part of horizontal turbulent mixing, transferring energy through a cascade of scale from large-scale movements to small-scale turbulence [6]. In recent years, special attention has been given to the study of eddy formation and frontogenesis at the meso- and submesoscale boundary in the Arctic seas [7, 8].

The climatic Polar Frontal Zone (PFZ) is located in the Barents Sea, the study of which is most often carried out according to contact observations [9, 10], because it is best observed on subsurface horizons. It is formed due to the advection of warm and salty Atlantic Water of the North Cape and Svalbard currents and their mixing with cold and desalinated Arctic Water [10, 11]. In the works [12, 13] this frontal zone is correlated with modified Barents Sea waters. It was found that the bottom topography plays an important role in the position of the PFZ [14–16]. The frontal zone in most works is defined only by temperature data [10, 17, 18], much less by salinity [4]. According to oceanographical measurements [17–19], the greatest thermal and salinity gradients inside the PFZ are observed in the area of Bear Island, which is associated with the closest contact of the Atlantic Water and Arctic Water. The study of the relationship between the position of the PFZ and the characteristics of the Arctic ice cover showed that in the years of minimum ice cover, the PFZ is much more northerly [5] than in the years when the ice cover of the Barents Sea is above average [20]. In work [21], a study of the long-term seasonal variability of the Polar front and its branches over many years, based on reanalysis data, showed the presence of intra-seasonal cycles of its spatial variability. At the time, most of the studies of the PFZ are fragmentary, which is due both to the difficulties of interpreting its synoptic and intra-monthly variability, and to the inhomogeneous of spatial distribution of gradients within the front. In addition, according to data [9], the availability of measurements of the eastern part of the Barents Sea in different seasons is much lower than the western one, making it impossible to fully describe the contribution of the PFZ to the hydrological regime of the entire Barents Sea. The use of modeled data and reanalysis does not always allow a qualitative description of the hydrophysical variability of the waters of the Barents Sea [22]. In this regard, a comprehensive study of the long-term variability of the PFZ using remote sensing data remains relevant.

A specific aspect is the choice of a methodological tool for the identification of frontal zones in the Arctic seas. The variety of techniques for identifying frontal zones in different parts of the World Ocean is associated with both regional features of frontogenesis and the data type used. In work [23], the frontal zone is defined as an area that is distinguished by a significant excess of the horizontal gradient over the background distribution. However, the instability of external boundaries and the highly variable gradient of frontal zones in the Arctic seas do not allow for a qualitative determination of the main characteristic and their variability at significant intervals. In addition, difficult weather conditions and ice cover, observed both in the warm [24] and in the cold period of the year [25], reduce the possibility of conducting regular assessment of the variability of the characteristic of the frontal zones of the Arctic by traditional methods such as oceanographical measurements. It should be noted that the PFZ in the Barents Sea is most pronounced in the 30–50 m [17] layer, while in the surface layer it is not always unambiguously detected. The solution may be the integration of satellite measurements of temperature and salinity of the sea surface with the identification of the frontal zone using the cluster analysis method [26].

At the boundaries of frontal zones, a variety of volatility mechanisms often create eddy structures of varying scales [27, 28]. It provides significant amounts of water transfer through the frontal zone. As a result, the frequency of times of occurrences of eddy structures indirectly reflects the intensity of water exchange between different areas. Satellite radar measurements (SAR) make it possible to effectively investigate the surface manifestations of small eddy struc-

tures at the borders and inside the frontal zones of the Arctic seas [19, 29]. However, the question remains as to how large-scale processes affect the intensity and spatial distribution of small eddy structures in the PFZ area. This is very important for understanding the features of water interaction processes in the frontal zone.

Atmospheric circulation over the North Atlantic and Barents Seas contributes significantly to the formation of thermohaline characteristics of waters in the region [30]. The work [30, 31] describes the relationship between Atlantic Water temperature in the Barents Sea and atmospheric oscillations. However, to date, no assessment has been made of the degree of correlation of the PFZ parameters in the surface layer with the indices of atmospheric fluctuations.

Thus, the purpose of this work is to study the spatial and temporal variability of PFZ characteristics in the surface layer of the Barents Sea between 2002 and 2020 and their correlation to the various processes in the atmosphere and the ocean.

2. Materials and methods

For the identification of surface PFZ, sea surface temperature (SST) data from the treatment level L3 [32] from May to September from 2002 to 2020 were used from MODIS (Moderate Resolution Imaging Spectroradiometer) satellite radiometers Aqua and Suomi NPP VIIRS (Visible Infrared Imaging Radiometer Suite) with a spatial resolution of 4 km [33, 34].

As data describing the variability of the salinity of the sea surface (SSS) inside the PFZ, data from the L3 processing level [35] of the NASA SMAP (Soil Moisture Active Passive) satellite for the period from June to September from 2016 to 2020 were taken with a spatial resolution of 0.25° in latitude and longitude [36].

After receiving the data, according to the methodology presented in work [37], the horizontal gradients of temperature and salinity characteristics were calculated. Further, the SST, SSS data and their gradients were combined into common matrices and brought to a single spatial grid using the linear interpolation method with a minimum step of 0.25° in latitude and longitude.

Matrices in which the number of omissions was more than 20 % were not used in further calculations.

To identify the PFZ on the surface of the Barents Sea, a cluster analysis [26, 38] of the combined data by the k-means method was performed. The standardization of each characteristic was done by dividing by the maximum value. The determination of the optimum number of classes was carried out by the Ward methods and tested by the criterion of minimization of the intra-class and inter-class distance ratios. For the class corresponding to the PFZ, the average values of SST, SSS and their gradients as well as the occupied area, were determined on the monthly and annual variability internal. To determine the position of the main Polar front inside the PFZ, the method of composite gradient maps with isolines SST and SSS described in detail in work [39], was used.

To record surface manifestations of eddy structures in the Barents Sea, 818 SAR Envisat Asar radar were analyzed in C-band and Wide Swath Mode (WSM) and Image Mode Precise (IMP) for August 2007 (197 images), 2009 (458 images) and 2011 (163 images). In August 2018, the analysis of 233 SAR Sentinel-1A and 1B radars in C-band and Interferometric Wide Swath (IW) and Extra Wide Swath (EW) was performed. The analysis of satellite radar and the separation of eddy structures were carried out according to the methodology described in the work [7]. To analyze the influence of wind on the manifestations of eddy structures the average monthly data on near-water wind speeds of GLOBAL OCEAN WIND L4 REPROCESSED MONTHLY MEAN OBSERVATION [40] were used, corresponding to front areas.

To assess the influence of large-scale atmospheric processes on the characteristics of the PFZ (such as: the prevailing directions of air mass transfer over the North Atlantic; the movement of synoptic-scale baric formations and their blocking processes over Europe), monthly average data were used of the indices of the North Atlantic Oscillation (NAO), East Atlantic Oscillation (EA), Scandinavian Oscillation (SCAND) and fluctuations of the Eastern Atlantic — Western Russia (EA/WR) [41] for the period from 2002 to 2020.

The estimate of the indices was averaged by the seasons of the year, and to determine the degree of relationship between the characteristics of the PFZ and atmospheric indices, the method of correlation analysis presented in the work was used [38].

3. Results

Polar frontal zone. Figure 1 shows as an example the results of cluster analysis based on monthly average satellite data in the Barents Sea for August 2018. According to the obtained static criteria (Fig. 1, *a*), the division of data into three classes is the most appropriate.

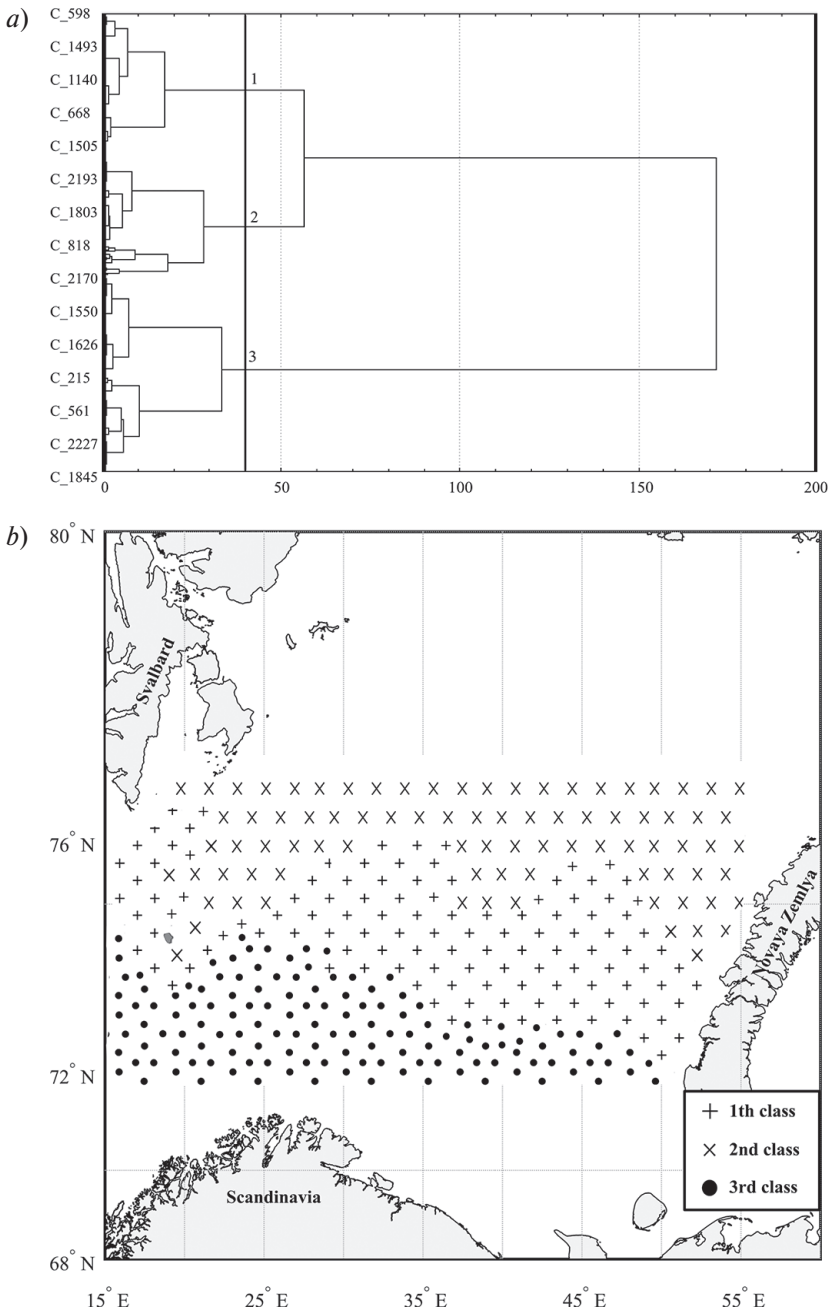

Fig. 1. Results of cluster analysis of average monthly SST, SSS and their gradients in August 2018.: *a* — dendrogram for determining the optimal number of classes obtained by the Ward method; *b* — classification obtained by k-means method: 1 class — PFZ region, 2 class — Arctic Water, 3 class — Atlantic Water.

The obtained clustering results when compared with other studies in term of thermohaline characteristics of the waters of the Barents Sea [9–11, 18, 42] show that the first-class correlates with the position (Fig. 1, *b*) and parameters (Table 1) PFZ: maximum SST gradient observed, the characteristics of SST and SSS are generally higher than their average values for the Barents Sea. The second class corresponds to the Arctic Water, with estimates comparable to the work [42]. For this water mass, the SSS gradient is elevated and the SST gradient is small. The third class is related to the Atlantic Water described in work [18] with maximum values of SST and SSS (Table 1).

As can be seen from Fig. 1, the PFZ originates near Bear Island, closer to the Svalbard archipelago. Here the PFZ is observed almost all year round, and in its region the maximum values of temperature and salinity are detected, due to flooding of warm and salty waters of the Svalbard Current [43, 44]. Then the zone goes around about Bear Island

and passes northeast along the Bear Island to 25° E. The direction of distribution of surface PFZ, depending on the year, can be divided into types: northern, when the PFZ is observed above 76° N and southern, when the area is below 72° N. The width of the region is subject to significant interannual variability.

The estimates of intra-annual variability of PFZ characteristics average over 2002–2020 are presented in Table 2. The table shows that the gradients of SST and SSS remain stable throughout the period under review. The temperature and salinity of the waters reflect the general trend of the annual course with a maximum in July–August. The surface area of the PFZ increases during the warm season, and a sharp increase is observed at the beginning of the season.

During the warm season, the SST in the PFZ region ranges from 1.5 °C in May to 8.5 °C in August (Fig. 2, see Inset), and SSS from 34.7 ‰ in June to 35.3 ‰ in October. The general temporal variability of SST is characterized by lower temperatures from 2003 to 2010, and after 2010, on the contrary, a warming trend is visible. On average, the difference between the first and second decades can reach 0.5–1.0 °C, which correlates with global trends in the changing climate in the Arctic [45].

The years with the minimum values of the SST gradient coincide with the periods in which intensive temperature anomalies of different signs were observed. In the first decade, the SST gradient was generally higher, and after 2010 there was a general downward trend in intensity with general warming in PFZ (Fig. 3). The maximum difference between decades is reached 0.04 °C/km and has tended to increase. It should also be noted that the maximum SST gradient values are cyclical, averaging 3–4 years.

The inter-annual variability of the SSS and the SSS gradients in the PFZ region is characterized by the maximum in 2018 and the minimum in 2020. No clear links with other PFZ parameters were found. It should also be noted, however, that the negative anomaly reported by SST in 2019 also appears in the lower SSS values.

PFZ area values are highly variable over decades. It can be seen that in the first decade of the 21st century, when SST values were on average lower, the PFZ covered a large part of the Barents Sea (Fig. 3), but after 2010, when total warming was observed, it was reduced by 50,000–80,000 km^2. The greatest positive anomalies in time in the area of the PFZ were observed in the warm seasons of 2008 and 2009, after 2007, when the area of the Arctic ice cover was much smaller than the average annual one [2]. In general, it should be noted that the maximum gradient values are observed when the area of PFZ is minimal and, conversely, when the area of the zone is maximum, the SST gradient in it is minimal. It can be seen that in the second decade of the 21st century there was a turning point in the variability of the PFZ area — it has decreased and its annual course ceased to have clear trends.

The maximum values of the gradient were more common in the first decade of the 21st century (Fig. 3). For example, the maximums were noted in 2002, 2003, 2006, 2010. The PFZ area is also characterized by maximums in the period from 2002 to 2010. Cold years with the gradient well below average can be attributed to 2005, 2008, 2016. The

Table 1

Intra-class monthly average estimates of the quantitative characteristic of SST, SSS and their gradients for August 2018: $\overline{T}$ — SST, $\Delta\overline{T}$ — SST gradient, $\overline{S}$ — SSS, $\Delta\overline{S}$ — SSS gradient, s — area.

Characteristic	1 class	2 class	3 class
$\overline{T}$, °C	7.2	4.7	10
$\Delta\overline{T}$, °C/km	0.07	0.05	0.06
$\overline{S}$, ‰	35.1	34.4	35.2
$\Delta\overline{S}$, ‰/km	0.016	0.034	0.007
s*10^3, km^2	311	338	268

Table 2

Intra-annual estimates of the quantitative characteristics of the PFZ for the period from May to September

Month	$\overline{T}$, °C	$\Delta\overline{T}$, °C/km	S, ‰	$\Delta\overline{S}$, ‰/km	s*10^3, km^2
May	2.61	0.05			245
June	3.71	0.05	34.91	0.02	288
July	5.75	0.05	35.02	0.02	313
August	6.74	0.04	34.97	0.02	331
September	5.97	0.05	34.92	0.02	341

analysis of the data shows that after 2010 the values of the SST gradients decreased markedly, which affected both the area of the frontal zone and the magnitude of its gradients. This is probably due to the "Atlantification" of the waters of the Barents Sea [3, 4], as a consequence of which the intensity of development on the surface of the PFZ decreases.

Eddies structures in the PFZ region. The number of eddy structures in the PFZ area by years can be estimated according to the data in Table 3, and Fig. 4 shows the spatial variability of eddies in the PFZ area in the years of their maximum and minimum occurrence in the water area.

It can be seen from Table 3 that the PFZ characteristics for the months are presented in Fig. 2. For example, with the minimum PFZ area in 2018, the maximum SST gradient is observed, and with the maximum area in 2009, the minimum. In addition, the variability between decades can be clearly traced according to the PFZ area data — in the first (2007, 2009) it is much higher than in the second (2011, 2018). Thus, August allows, in general terms, to trace the dynamics of the PFZ during the periods of its maximum variability.

According to Table 3, the number of registered eddy structures differs from each other by years in the sea as a whole and the frontal zone. A clear criterion for the occurrence of eddies is the radio of the number of eddies inside the PFZ and the number of eddies in the remaining area of the Barents Sea. The close value of the criterion to 0 shows that eddies prevail in the Barents Sea, and at a value close to 1, that eddies prevail in the PFZ area. The criterion shows the frequent occurrence of eddies in the PFZ in 2009 and very low in 2007 and 2018. However, this criterion does not allow for an understanding under the influence of which factors in the PFZ region eddies appear. Note that in those years when the average monthly wind speed in the PFZ did not exceed 6 m/s the eddy structures inside the PFZ were recorded much more frequently compared to years with higher average wind speeds.

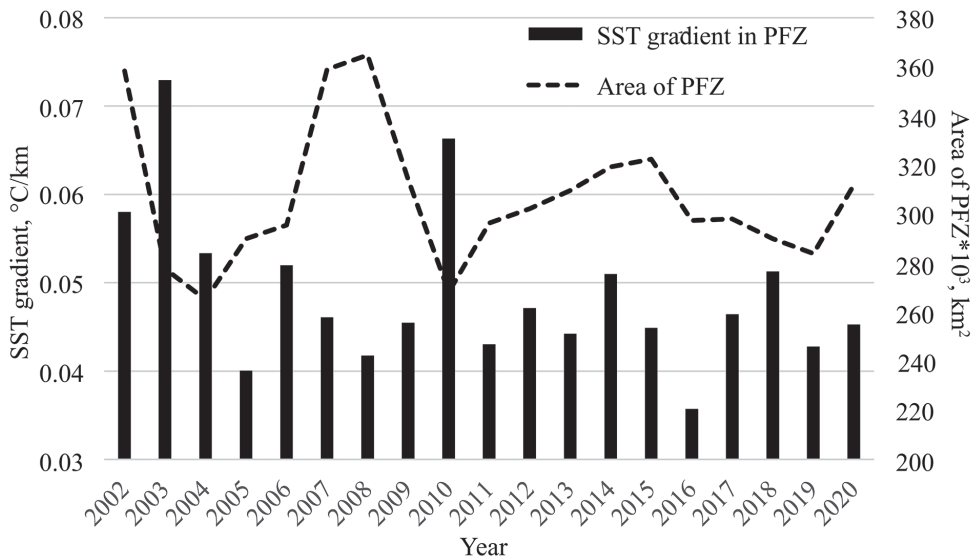

Fig. 3. Average annual estimates of the SST and the PFZ area.

Table 3

Main characteristics and statistical criteria of eddy structures in the PFZ and characteristics of wind speeds in the PFZ region.

Year	2007	2009	2011	2018
Number of eddies, units	366	613	194	665
Average diameter, km	2.3	6.5	2.7	3.1
Number of eddies in the PFZ region, units	12	113	25	29
The ratio of the number of eddies to the number of SAR (repeatability)	1.85	1.33	1.19	2.98
The ratio of the number of eddies inside the PFZ and outside the PFZ units/1*10^3 km^2	0.06	0.61	0.43	0.14
PFZ width, thousand km^2	345	380	328	312
Maximum gradient, °C/km	0.05	0.04	0.04	0.07
Median, °C/km	0.032	0.027	0.026	0.034
Maximum wind speed in the PFZ area, m/sec	6.62	5.92	5.05	7.26

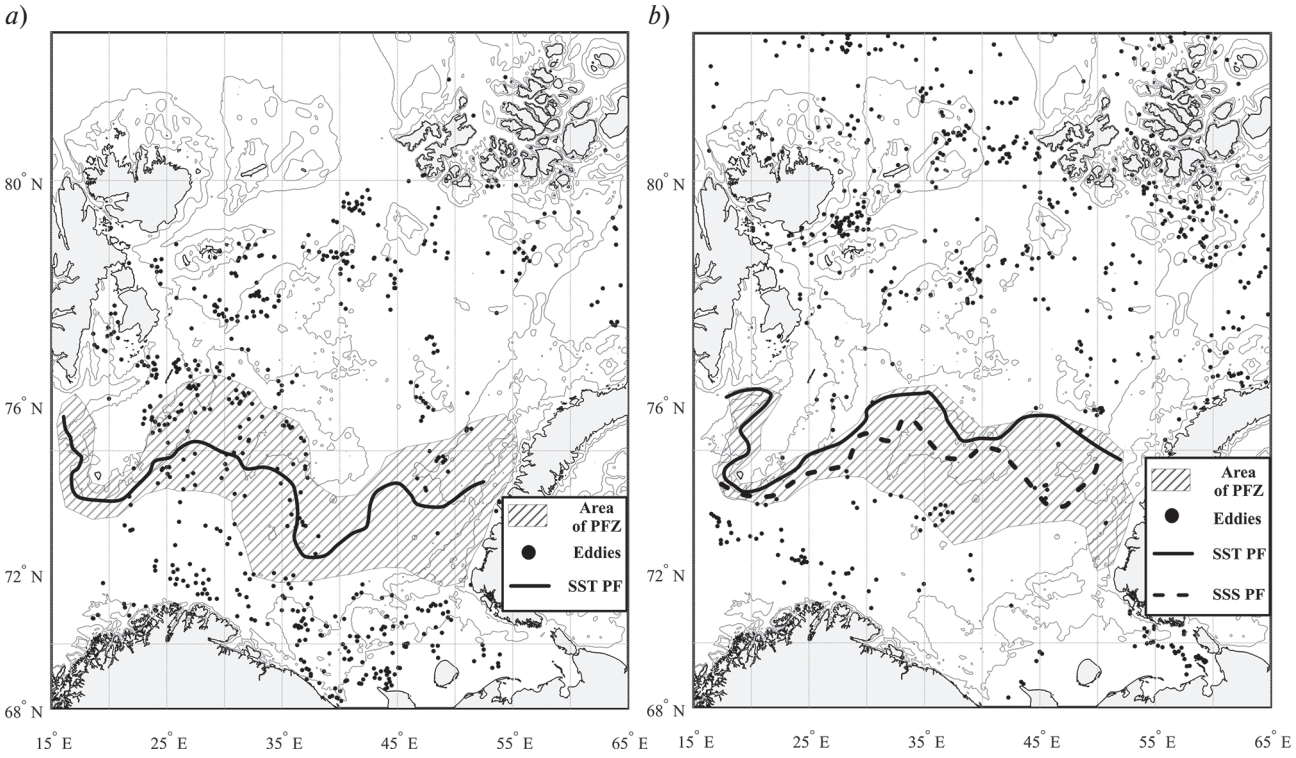

Fig. 4. Composite maps of the PFZ according to SST, SSS and eddy structures for August: *a* — 2009; *b* — 2018.

Figure 4 illustrates the inhomogeneity of the distribution of eddies in the Barents Sea in different years. In 2007 and 2018, the main areas of occurrence are located in the northern part of the sea, closer to the Svalbard and France Josef Land archipelagos, in 2009 and 2011, many eddy structures are located in the central and southern parts of the Barents Sea. It is also should be noted structures are often found in areas with significant variability in bottom topography (for example, near the Central Bank).

An analysis of the obtained results shows that the maximum eddy formation from the presented years in the field of PFZ was observed in August 2009. This is probably due to the small values of the SST gradient, which increases the probability of the development of baroclinic instability [6] in the PFZ. This is also confirmed by statistical criteria: small values of dispersion and median, which show that the variation in the SST gradient is insignificant. In addition, moderate wind exposure can contribute not only to the intensification of dynamic processes, but also to better identification of the PFZ eddy patterns in satellite imagery.

Atmospheric oscillations. A comparison of the temporal variability of PFZ characteristic indices showed that an increase in the SST of the Barents Sea is observed in the same years as an increase in the NAO and EA indices. In some years, there are simultaneous maxima of the SCAND indices and SST gradients. There are also feedbacks when in the first decade PFZ values are maximal, NAO, EA and SCAND indices are generally lower. There is no clear correlation between the time variability of EA/WR indices and PFZ characteristics.

The resulting statistical estimates of the correlation between the seasonal characteristics of PFZ and the indices of global atmospheric processes are presented in Table 4.

According to the results obtained, the greatest connection is observed between SCAND and the characteristics of the PFZ with a shift of six months. The change in the Scandinavian fluctuation in winter can describe up to 47 % of the variability of the PFZ characteristics in the next summer season (Table 4). With positive values of the index, an increase in anticyclonic activity occurs [46–48], which enhances energy exchange with the atmosphere. As a result of an increase in heat transfer from the ocean to the atmosphere in the winter season, convective processes in the active layer of the Norwegian Sea are intensified. In the future, these waters are transported to the Barents Sea and, being colder, they sink faster and form a smaller area on the surface, but more pronounced gradients in the PFZ region.

Significant correlation coefficients of winter EA/WR indices are observed only with the parameters of the PFZ area. This may be due to the zonal transfer of warm air masses from Eurasia, which may indirectly affect the heat content of waters in the Barents Sea and, as a result, increase the area of the PFZ [49, 50].

No significant correlation between atmospheric circulation indices and PFZ characteristic were found in the spring period. Summer atmospheric circulation indices EA correlate with SST characteristics in the PFZ region.

Table 4

Correlation coefficients between PFZ characteristics and NAO, EA, EA/WR and SCAND indices by seasons for 2002–2020. Correlation coefficients significant at the 95 % level are highlighted in bold.

Parameter	NAO	EA	EA/WR	SCAND
Winter indexes — summer characteristics of PFZ				
T	0.26	0.18	–0.01	**–0.42**
ΔT	–0.39	0.06	–0.05	**0.47**
s	0.20	–0.20	**0.42**	**–0.44**
Spring indexes — summer characteristics of PFZ				
T	0.39	0.13	0.33	–0.15
ΔT	–0.04	–0.01	0.14	0.16
s	0.13	–0.07	0.06	–0.24
Summer indexes — summer characteristics of PFZ				
T	0.36	**–0.43**	0.01	0.11
ΔT	0.23	–0.11	–0.25	0.33
s	–0.08	–0.33	0.11	0.13

The reverse character of the latter relationship is possibly explained by the fact that, with the intensification of the meridional circulation over the northern part of the Atlantic Ocean, there is an intensification of the transfer of cold air masses and a decrease in the SST in the PFZ region [51].

The values of the correlation coefficients between the characteristics of PFZ and NAO presented in Table 4 are comparable with the estimates from work [52]. The size of the shift and the correlation coefficients of the SCAND index are similar to the results of work [48], where its influence on the change and formation of the ice cover of the Barents and Kara Seas is described.

The results allow the possibility of using a winter index to be considered as a predictor for predicting the characteristics of the surface PFZ for the next summer season. At the same time, the absolute values of the correlation coefficients are generally not large, which shows the importance of regional atmospheric and hydrological processes in the formation of the PFZ in the Barents Sea.

4. Conclusion

In the course of this work, the spatial and temporal variability of PFZ characteristics in the Barents Sea for the period from 2002 to 2020 was investigated. The analysis of the interannual variability of eddy structures repeatability near the frontal zone and the connection of characteristics of PFZ with global atmospheric processes is performed.

An analysis of the annual average characteristics of the PFZ showed that the gradients of the SST and the SSS were quite stable, while its area experienced significant changes at the beginning of the summer season. The maximum value of the SST was in 2013, the PFZ gradient in 2003 and the PFZ area in 2007. The minimum values of SST characteristics and PFZ area were observed in 2003 and the SST gradient in 2015. The inter-annual and seasonal variability of PFZ characteristics showed that its intensity in the first decade was on an order of magnitude higher than in the period 2011–2020. This is confirmed by the estimates of the SST gradient and the area of the PFZ, which so far show a negative trend. This trend is likely related to the increased flooding of warm Atlantic Water in the Barents Sea, which creates positive SST anomalies while destabilizing the sustainability of the PFZ.

Analysis of PFZ eddies shows that the maximum number of eddy structures was observed in August 2009. In other years, there is no similar spatial distribution of eddies in the PFZ region. This is probably due to the development of a more intense barocline instability this year, resulting from the weakening of the performance gradients in the PFZ. This assumption is confirmed by the small value of the median and dispersion of the SST gradient. It is also important to note here that the possible reasons for the registration of a larger number of eddies in satellite data in August 2009 may be a better provision of observations (a larger number of radar images obtained in the PFZ region) and more favorable wind conditions under which the identification of eddies in radar images is optimal.

The results of the analysis of the statistical correlation between the characteristics of the front and the seasonal indices of atmospheric circulation show that the variability of the PFZ characteristics in the summer season is best described by the SCAND index for the previous winter. It is shown that an increase in anticyclonic activity over the Scandinavian Peninsula can affect an increase in SST gradients and a decrease in the area of the surface PFZ. The results obtained will further allow to develop a new approach to predicting the characteristics of the PFZ.

Further work will focus on the internal structure and synoptic variability of PFZ characteristics in years with different climatic conditions.

5. Funding

This research was supported by RFBR grant 20–35–90053 (analysis of the data on frontal zone characteristic and atmospheric oscillations); the Ministry of Science and Higher Education of the Russian Federation, theme 0128–2021–0014 (processed and analyzed of satellite data on sea surface temperature and salinity); the Ministry of Science and Higher Education of the Russian Federation, theme 075–00429–21–03 (analysis of the characteristics of eddies structures according to satellite SAR data).

Литература

1. *Трофимов А.Г.*, *Карсаков А.Л.*, *Ившин В.А.* Изменения климата в Баренцевом море на протяжении последнего полувека // Труды ВНИРО. 2018. Т. 173. С. 79–91.
2. *Feltham D.* Arctic Sea ice reduction: the evidence, models and impacts // Philos Trans. R. Soc. A Math. Phys. Eng. Sci. 2015. V. 373, N 2045. P. 20140171. doi: 10.1098/rsta.2014.0171
3. *Årthun M.*, *Eldevik T.*, *Smedsrud L.H.*, *Skagseth Ø.*, *Ingvaldsen R.B.* Quantifying the influence of Atlantic heat on Barents Sea ice variability and retreat // J. Climate. 2012. V. 25, N 13. P. 4736–4743. doi: 10.1175/jcli-d-11–00466.1
4. *Barton B.I.*, *Lenn Y.D.*, *Lique C.* Observed Atlantification of the Barents Sea causes the Polar front to limit the expansion of winter sea ice // J. Phys. Oceanogr. 2018. V. 48, N 8. P. 1849–1866. doi: 10.1175/jpo-d-18–0003.1
5. *Атаджанова О.А.*, *Зимин А.В.*, *Свергун Е.И.*, *Коник А.А.* Субмезомасштабные вихревые структуры и фронтальная динамика в Баренцевом море // Морской гидрофизический журнал. 2018. Т. 34, № 3. С. 237–246. doi: 10.22449/0233–7584–2018–3–237–246
6. *Костяной А.Г.*, *Лебедев И.А.*, *Новиков В.Б.*, *Родионов В.Б.* О вихреобразовании в Полярной фронтальной зоне Баренцева моря // Труды ААНИИ. 1992. Т. 426. С. 19–32.
7. *Kozlov I.E.*, *Artamonova A.V.*, *Manucharyan G.E.*, *Kubryakov A.A.* Eddies in the Western Arctic Ocean from spaceborne SAR observations over open ocean and marginal ice zones // J. Geophys. Res. Oceans. 2019. V. 124, N 9. P. 6601–6616. doi: 10.1029/2019jc015113
8. *Родионов А.А.*, *Романенков Д.А.*, *Зимин А.В.*, *Козлов И.Е.*, *Шапрон Б.* Субмезомасштабные структуры вод Белого моря и их динамика. Состояние и направления исследований // Фундаментальная и прикладная гидрофизика. 2014. Т. 7, № 3. С. 29–41.
9. *Ожигин В.К.*, *Ившин В.А.*, *Трофимов А.Г.*, *Красаков А.Л.*, *Анциферов М.Ю.* Воды Баренцева моря: структура, циркуляция, изменчивость. Мурманск: ПИНРО, 2016. 260 с.
10. *Oziel L.*, *Sirven J.*, *Gascard J.C.* The Barents Sea frontal zones and water masses variability (1980–2011) // Ocean Sci. 2016. V. 12, N 1. P. 169–184. doi: 10.5194/os-12–169–2016
11. *Добровольский А.Д.*, *Залогин Б.С.* Моря СССР. М.: МГУ, 1982. 192 с.
12. *Чвилев С.В.* Фронтальные зоны Баренцева моря // Метеорология и гидрология. 1991. № 11. С. 103–108.
13. *Harris C.L.*, *Pluedemann A.J.*, *Gawarkiewich G.G.* Water mass distribution and polar front structure in the western Barents Sea // J. Geophys. Res. Oceans. 1998. V. 103, N C2. P. 2905–2917. doi: 10.1029/97jc02790
14. *Johannessen O.M.*, *Foster L.A.* A note on the topographically controlled oceanic polar front in the Barents Sea // J. Geophys. Res. 1978. V. 83, N C9. P. 4567–4571. doi: 10.1029/jc083ic09p04567
15. *Reynolds R.W.*, *Rayner N.A.*, *Smith T.M.*, *Stokes D.C.*, *Wang W.* An improved in situ and satellite SST analysis for climate // J. Climate. 2002. V. 15. P. 1609–1625.
16. *Parsons A.R.*, *Bourke R.H.*, *Muench R.D.*, *Chiu C.— S.*, *Lynch J.F.*, *Miller J.H.*, *Plueddemann A.J.*, *Pawlowicz R.* The Barents Sea polar front in summer // J. Geophys. Res. 1996. V. 101, N C6. P. 14201–14221. doi: 10.1029/96jc00119
17. *Ivshin V.A.*, *Trofimov A.G.*, *Titov O.V.* Barents Sea thermal frontal zones in 1960–2017: variability, weakening, shifting // ICES J. Mar. Sci. 2019. V. 76, Issue Supplement 1. P. i3—i9. doi: 10.1093/icesjms/fsz159
18. *Våge S.*, *Basedow S.L.*, *Tande K.S.*, *Zhou M.* Physical structure of the Barents Sea Polar Front near Storbanken in August 2007 // J. Mar. Syst. 2014. V. 130. P. 256–262. doi: 10.1016/j.jmarsys.2011.11.019
19. *Fer I.*, *Drinkwater K.* Mixing in the Barents Sea Polar Front near Hopen in spring // J. Mar. Syst. 2014. N 130. P. 206–218. doi: 10.1016/j.jmarsys.2012.01.005
20. *Коник А.А.*, *Козлов И.Е.*, *Зимин А.В.*, *Атаджанова О.А.* Спутниковые наблюдения вихрей и фронтальных зон Баренцева моря в годы с различной ледовитостью // Современные проблемы дистанционного зондирования Земли из космоса. 2020. Т. 17, № 5. С. 191–201. doi: 10.21046/2070–7401–2020–17–5–191–201
21. *Артамонов Ю.В.*, *Скрипалева В.А.*, *Федирко А.В.* Сезонная изменчивость температурных фронтов на поверхности Баренцева моря // Метеорология и гидрология. 2019. № 1. С. 78–89.

22. *Зимин А.В.*, *Атаджанова О.А.*, *Коник А.А.*, *Гордеева С.М.* Сравнение результатов наблюдений, выполненных в Баренцевом море, с данными из глобальных океанологических баз // Фундаментальная и прикладная гидрофизика. 2020. Т. 13, № 4. С. 66–77. doi: 10.7868/S2073667320040061
23. *Федоров К.Н.* Физическая природа и структура океанических фронтов. Л.: Гидрометеоиздат, 1983. 296 с.
24. *Бардин М.Ю.*, *Платова Т.А.*, *Самохина О.Ф.* Особенности изменчивости циклонической активности в умеренных широтах северного полушария, связанные с ведущими модами атмосферной циркуляции в атлантико–европейском секторе // Фундаментальная и прикладная климатология. 2015. Т. 2. С. 14–40.
25. *Золотокрылин А.Н.*, *Титкова Т.Б.*, *Михайлов А.Ю.* Климатические вариации арктического фронта и ледовитости Баренцева моря зимой // Лед и снег. 2014. Т. 54, № 1. С. 85–90.
26. *Вайновский П.А.*, *Малинин В.Н.* II. Методы обработки и анализа океанологической информации. Многомерный анализ. Учебное пособие. СПб.: РГГМИ, 1992. 96 с.
27. *Ikeda M.*, *Johannessen J.A.*, *Lygre K.*, *Sandven S.* A process study of mesoscale meandres and eddies in the Norwegian Coastal Current // J. Geophys. Res. 1989. V. 19, N 1. P. 20–35. doi: 10.1175/1520–0485(1989)019<0020: APSOMM>2.0.CO;2
28. *Manucharyan G.E.*, *Timmermans M.L.* Generation and separation of mesoscale eddies from surface ocean fronts // J. Phys. Oceanogr. 2014. V. 43, N 12. P. 2545–2562. doi: 10.1175/jpo-d-13–094.1
29. *Атаджанова О.А.*, *Зимин А.В.*, *Романенков Д.А.*, *Козлов И.Е.* Наблюдение малых вихрей в Белом, Баренцевом и Карском морях по данным спутниковых радиолокационных измерений // Морской гидрофизический журнал. 2017. № 2. С. 75–83. doi: 10.22449/0233–7584–2017–2–80–90
30. *Алексеев Г.В.*, *Глок Н.И.*, *Смирнов А.Е.*, *Вязилова А.Е.* Влияние Северной Атлантики на колебания климата в районе Баренцева моря и их предсказуемость // Метеорология и гидрология. 2016. Т. 41, № 8. С. 83–56.
31. *Schlichtholz P.*, *Houssais M.N.* Forcing of oceanic heat anomalies by air–sea interactions in the Nordic seas area // J. Geophys. Res. 2011. V. 116., N C01006. doi: 10.1029/2009jc005944
32. NASA's OceanColor Web [Электронный ресурс]. URL: http://oceancolor.gsfc.nasa.gov (дата обращения: 04.06.2021).
33. *Li Na*, *Li Bingrui*, *Lei Ruibo*, *Li Qun*. Comparison of summer Arctic Sea ice surface temperatures from in situ and MODIS measurements // Acta Oceanologica Sinica. 2020. V. 9, N 39. P. 18–24.
34. *Liu Y.*, *Minnett P.J.* Sampling errors in satellite–derived infrared sea–surface temperatures. Part I: Global and regional MODIS fields // Remote Sens. Environ. 2016. V. 177. P. 48–64. doi: 10.1016/j.rse.2016.02.026
35. The Physical Oceanography Distributed Active Archive Center [Электронный ресурс]. URL: https://podaac.jpl.nasa.gov (дата обращения: 04.06.2021).
36. *Meissner T.*, *Wentz F.J.*, *Le Vine D.M.* The Salinity Retrieval Algorithms for the NASA Aquarius Version 5 and SMAP Version 3 Releases // Remote Sens. 2018. N 10. P. 1121. doi: 10.3390/rs10071121
37. *Ожигин В.К.* Термические фронтальные зоны Баренцева моря и особенности распределения скоплений промысловых рыб // Вопросы промысловой океанологии Северного бассейна: сб. науч. тр. ПИНРО.: Мурманск, 1989. С. 104–117.
38. *Гордеева С.М.*, *Малинин В.Н.* Крупномасштабная изменчивость южного субтропического фронта в юго-восточной части Тихого океана // Ученые записки РГГМУ. 2006. № 2. С. 160–169.
39. *Коник А.А.*, *Зимин А.В.*, *Атаджанова О.А.* Количественные оценки изменчивости характеристик температуры поверхности моря в районе фронтальных зон Карского моря // Фундаментальная и прикладная гидрофизика. 2019. Т. 12, № 1. С. 54–61. doi: 10.7868/S2073667319010076
40. Copernicus Marine Environment Monitoring Service. GLOBAL OCEAN WIND L4 REPROCESSED MONTHLY MEAN OBSERVATIONS [Электронный ресурс]. URL: https://resources.marine.copernicus.eu (дата обращения: 04.06.2021).
41. Climate Prediction Center [Электронный ресурс]. URL: http://www.cpc.ncep.noaa.gov (дата обращения: 04.06.2021).
42. *Гирдюк Г.В.*, *Дженюк С.Л.*, *Зыкова Г.Г.*, *Терзиев Ф.С.* Гидрометеорология и гидрохимия морей СССР. Том 1. Баренцево море. Выпуск 1. Гидрометеорологические условия. Ленинград: Гидрометеоиздат, 1990. С. 280.
43. *Parsons A.R.*, *Bourke R.H.*, *Muench R.D.*, *Chiu C.-S.*, *Lynch J.F.*, *Miller J.H.*, *Plueddeman A.J.*, *Pawlowicz R.* The Barents Sea Polar Front in summer // J. Geophys. Res.: Oceans. 1996. V. 101, N C6. P. 14201–14221. doi: 10.1029/96jc00119
44. *Соколов А.А.*, *Гордеева С.М.* Изменение адвекции тепла в Баренцевом море // Российская Арктика. 2019. № 4. С. 34–44.
45. *Timmermans M.L., Labe Z.* Arctic Report Card 2020: Sea Surface Temperature // NOAA Arctic Report Card 2020. 2020. P. 1–5. doi: 10.25923/v0fs-m920
46. *Drinkwater K.F.*, *Mueter F.*, *Friedland K.D.*, *Taylor M.*, *Hunt G.L.*, *Hare J.*, *Melle W.* Recent climate forcing and physical oceanographic changes in Northern Hemisphere regions: A review and comparison of four marine ecosystems // Prog. Oceanogr. 2009. V. 81, N 1–4. P. 10–28. doi: 10.1016/j.pocean.2009.04.003

47. *Суркова Г.В.*, *Романенко В.А.* Баренцево море: сезонная и многолетняя изменчивость энергообмена с атмосферной // Материалы научной конференции «Моря России: исследование береговой и шельфовых зон». Севастополь, 21–25 сентября 2020 года. Севастополь: МГИ, 2020. С. 187–188.

48. *Попова В.В.* Вклад аномалий ледяного покрова Баренцева и Карского морей в изменение режима циркуляции и температуры северной Евразии с середины 1990–х годов // Лед и снег. 2020. Т. 60, № 3. С. 409–422.

49. *Rodriguez-Puebla C.*, *Encinas A.H.*, *Nieto S.*, *Garmendia J.* Spatial and temporal patterns of annual precipitation variability over the Iberian Peninsula // Int. J. Climatol. 1998. V. 18, N 3. P. 299–316. doi: 10.1002/(sici)1097–0088(19980315)18:3<299:: aid-joc247>3.0.co;2-1

50. *Нестеров Е.С.* Североатлантическое колебание: атмосфера и океан. М.: Триада ЛТД, 2013. 144 с.

51. *Виноградова А.А.* Сезонные и долговременные вариации индексов атмосферной циркуляции и перенос воздуха в Российскую Арктику // Оптика атмосферы и океана. 2014. Т. 27, № 6. С. 463–472.

52. *Ozhigin V.K.*, *Drobysheva S.S.*, *Ushakov N.G.* Internnual variability in the physical environment, zooplankton, capelin (Mllotus villosus) and North–East Arctic cod (Gadus morhua) in the Barents Sea // ICES Mar. Sci. Symposia. 2003. V. 219. P. 283–293.

References

1. *Trofimov A.G.*, *Karsakov A.L.*, *Ivshin V.A.* Climate changes in the Barents Sea over the last half century. *Trudy VNIRO*. 2018, 173, 79–91 (in Russian).

2. *Feltham D.* Arctic Sea ice reduction: the evidence, models and impacts. *Philos Trans. R. Soc. A Math. Phys. Eng. Sci*.2015, 373, 2045, 20140171. doi: 10.1098/rsta.2014.0171

3. *Årthun M.*, *Eldevik T.*, *Smedsrud L.H.*, *Skagseth Ø.*, *Ingvaldsen R.B.* Quantifying the Influence of Atlantic Heat on Barents Sea Ice Variability and Retreat*. *J. Climate*. 2012, 25, 13, 4736–4743. doi: 10.1175/jcli-d-11–00466.1

4. *Barton B.I.*, *Lenn Y.D.*, *Lique C.* Observed Atlantification of the Barents Sea causes the Polar Front to limit the expansion of winter sea ice. *J. Phys. Oceanogr*. 2018, 48, 8, 1849–1866. doi: 10.1175/jpo-d-18–0003.1

5. *Atadzhanova O.A.*, *Zimin A.V.*, *Svergun E.I., Konik A.A.* Sub-Mesoscale Eddy structures and frontal dynamics in the Barents Sea. *Phys Oceanogr*. 2018, 34, 3, 237–246. doi: 10.22449/1573–160X-2018–3–220–228

6. *Kostjanoj A.G.*, *Lebedev I.A.*, *Novikov V.B.*, *Rodionov V.B.* On eddies formation in the Polar frontal zone of the Barents Sea. *Trudy AANII*. 1992, 426, 19–32 (in Russian).

7. *Kozlov I.E.*, *Artamonova A.V.*, *Manucharyan G.E.*, *Kubryakov A.A.* Eddies in the Western Arctic Ocean from spaceborne SAR observations over open ocean and marginal ice zones. *J. Geophys. Res.*: *Oceans*. 2019, 124, 9, 6601–6616. doi: 10.1029/2019jc015113

8. *Rodionov A.A.*, *Romanenkov D.A.*, *Zimin A.V.*, *Kozlov I.E., Shapron B.* Submesoscale processes and dynamics in the White Sea. State of the art and future research. *Fundam. Prikl. Gidrofiz*. 2014, 7, 3, 29–41 (in Russian).

9. *Ozhigin V.K.*, *Ivshin V.A.*, *Trofimov A.G.*, *Krasakov A.L.*, *Anciferov M. Ju.* The Barents Sea Water: structure, circulation, variability. *Murmansk*, *PINRO*, 2016. 260 p. (in Russian).

10. *Oziel L.*, *Sirven J.*, *Gascard J.C.* The Barents Sea frontal zones and water masses variability (1980–2011). *Ocean Sci.* 2016, 12, 1, 169–184. doi: 10.5194/os-12–169–2016

11. *Dobrovol'skij A.D.*, *Zalogin B.S.* Seas of the USSR. *Moscow*, *MSU*, 1982. 192 p. (in Russian).

12. *Chvilev S.V.* Frontal zones of the Barents Sea. *Meteorologija i Gidrologija*. 1991, 11, 103–108 (in Russian).

13. *Harris C.L.*, *Pluedemann A.J.*, *Gawarkiewich G.G.* Water mass distribution and polar front structure in the western Barents Sea. *J. Geophys. Res*: *Oceans*. 1998, 103, C2, 2905–2917. doi: 10.1029/97jc02790

14. *Johannessen O.M.*, *Foster L.A.* A note on the topographically controlled oceanic polar front in the Barents Sea. *J. Geophys. Res.* 1978, 83, C9, 4567–4571. doi: 10.1029/jc083ic09p04567

15. *Reynolds R.W.*, *Rayner N.A.*, *Smith T.M.*, *Stokes D.C.*, *Wang W.* An improved in situ and satellite SST analysis for climate. *J. Climate*. 2002, 15, 1609–1625.

16. *Parsons A.R.*, *Bourke R.H.*, *Muench R.D.*, *Chiu C.— S.*, *Lynch J.F.*, *Miller J.H.*, *Plueddemann A.J.*, *Pawlowicz R.* The Barents Sea polar front in summer. *J. Geophys. Res.* 1996, 101, C6, 14201–14221. doi: 10.1029/96jc00119

17. *Ivshin V.A.*, *Trofimov A.G.*, *Titov O.V.* Barents Sea thermal frontal zones in 1960–2017: variability, weakening, shifting. *ICES J. Mar. Sci.* 2019, 76, i3—i9. doi: 10.1093/icesjms/fsz159

18. *Våge S.*, *Basedow S.L.*, *Tande K.S.*, *Zhou M.* Physical structure of the Barents Sea Polar Front near Storbanken in August 2007. *J. Mar. Syst*. 2014, 130, 256–262. doi: 10.1016/j.jmarsys.2011.11.019

19. *Fer I.*, *Drinkwater K.* Mixing in the Barents Sea Polar Front near Hopen in spring. *J. Mar. Syst*. 2014, 130, 206–218. doi: 10.1016/j.jmarsys.2012.01.005

20. *Konik A.A.*, *Kozlov I.E.*, *Zimin A.V.*, *Atadzhanova O.A.* Satellite observations of eddies and frontal zones in the Barents Sea during years of different ice cover properties. *Sovr. Probl. DZZ Kosm*. 2020, 17, 5, 191–201 (in Russian). doi: 10.21046/2070–7401–2020–17–5–191–201
21. *Artamonov Ju.V.*, *Skripaleva V.A.*, *Fedirko A.V.* Seasonal Variability of Temperature Fronts on the Barents Sea Surface. *Russ. Meteorol. Hydrol.* 2019, 44, 53–61doi: 10.3103/S1068373919010060
22. *Zimin A.V.*, *Atadzhanova O.A.*, *Konik A.A.*, *Gordeeva S.M.* Comparison of hydrography observations with data of global products in the Barents Sea. *Fundam. Prikl. Gidrofiz*. 2020, 13, 4, 66–77 (in Russian). doi: 10.7868/S2073667320040061
23. *Fedorov K.N.* The physical nature and structure of oceanic fronts. *Leningrad*, *Gidrometeoizdat*, 1983. 296 p. (in Russian).
24. *Bardin M. Ju.*, *Platova T.A.*, *Samohina O.F.* Specific features of variability of cyclone activity in northern extratropics associated with leading atmospheric circulation modes in atlantic-european sector. *Fundamental and Applied Climatology*. 2015, 2, 14–40 (in Russian).
25. *Zolotokrylin A.N.*, *Titkova T.B.*, *Mihajlov A. Ju.* Climatic variations of the Arctic front and the Barents Sea ice cover in winter time. *Led i Sneg*. 2014, 54, 1, 85–90 (in Russian).
26. *Vajnovskij P.A.*, *Malinin V.N.* Methods of processing and analysis of oceanological information. Multidimensional analysis. Study guide. *St. Petersburg*, *RGGMI*, 1992. 96 p. (in Russian).
27. *Ikeda M.*, *Johannessen J.A.*, *Lygre K.*, *Sandven S.* A process study of mesoscale meandres and eddies in the Norwegian Coastal Current. *J. Geophys. Res*. 1989, 19, 1, 20–35. doi: 10.1175/1520–0485(1989)019<0020: APSOMM>2.0.CO;2
28. *Manucharyan G.E.*, *Timmermans M.L.* Generation and separation of mesoscale eddies from surface ocean fronts. *J. Phys. Oceanogr.* 2014, 43, 12, 2545–2562. doi: 10.1175/jpo-d-13–094.1
29. *Atadzhanova O.A.*, *Zimin A.V.*, *Romanenkov D.A.*, *Kozlov I.E.* Satellite radar observations of small eddies in the White, Barents and Kara Seas. *Phys. Oceanogr*. 2017, 2, 75–83. doi: 10.22449/1573–160X-2017–2–75–83
30. *Alekseev G.V.*, *Glok N.I.*, *Smirnov A.V.*, *Vyazilova A.E.* The influence of the North Atlantic on climate variations in the Barents Sea and their predictability. *Russ. Meteorol. Hydrol*. 2016, 41, 8, 544–558. doi: 10.3103/S1068373916080045
31. *Schlichtholz P.*, *Houssais M.N.* Forcing of oceanic heat anomalies by air–sea interactions in the Nordic seas area. *J. Geophys. Res*. 2011, 116, C01006. doi: 10.1029/2009jc005944
32. NASA's OceanColor Web URL: http://oceancolor.gsfc.nasa.gov (date of access: 04.06.2021).
33. *Li Na*, *Li Bingrui*, *Lei Ruibo*, *Li Qun*. Comparison of summer Arctic Sea ice surface temperatures from in situ and MODIS measurements. *Acta Oceanologica Sinica*. 2020, 9, 39, 18–24. doi: 10.1007/s13131–020–1644–7
34. *Liu Y.*, *Minnett P.J.* Sampling errors in satellite–derived infrared sea–surface temperatures. Part I: Global and regional MODIS fields. *Remote Sens. Environ*. 2016, 177, 48–64. doi: 10.1016/j.rse.2016.02.026
35. The Physical Oceanography Distributed Active Archive Center. URL: https://podaac.jpl.nasa.gov (date of access: 04.06.2021).
36. *Meissner T.*, *Wentz F.J.*, *Le Vine D.M.* The Salinity Retrieval Algorithms for the NASA Aquarius Version 5 and SMAP Version 3 Releases. *Remote Sens*. 2018, 10, 1121. doi: 10.3390/rs10071121
37. *Ozhigin V.K.* Thermal frontal zones of the Barents Sea and features of distribution of commercial fish aggregations. *Voprosy Promyslovoj Okeanologii Severnogo Bassejna: sb. nauch. tr. PINRO, Murmansk*, 1989, 104–117 (in Russian).
38. *Gordeeva S.M.*, *Malinin V.N.* Large-scale variability of the southern subtropical front in the south-eastern part Pacific Ocean. *Uchenye Zapiski RGGMU*. 2006, 2, 160–169 (in Russian).
39. *Konik A.A.*, *Zimin A.V.*, *Atadzhanova O.A.* Quantitative estimations of the variability of characteristics of the temperature of the sea surface in the front of the frontal zone of the Kara Sea. *Fundam Prikl Gidrofiz*. 2019, 12, 1, 54–61 (in Russian). doi: 10.7868/S2073667319010076
40. Copernicus Marine Environment Monitoring Service. GLOBAL OCEAN WIND L4 REPROCESSED MONTHLY MEAN OBSERVATIONS. URL: https://resources.marine.copernicus.eu (date of access: 04.06.2021).
41. Climate Prediction Center. URL: http://www.cpc.ncep.noaa.gov (date of access: 04.06.2021).
42. *Girdjuk G.V.*, *Dzhenjuk S.L.*, *Zykova G.G.*, *Terziev F.S.* Hydrometeorology and hydrochemistry of the seas of the USSR. V. 1. The Barents Sea. Issue 1. Hydrometeorological conditions. *Leningrad*, *Gidrometeoizdat*, 1990. 280 p. (in Russian).
43. *Parsons A.R.*, *Bourke R.H.*, *Muench R.D.*, *Chiu C.— S.*, *Lynch J.F.*, *Miller J.H.*, *Plueddeman A.J.*, *Pawlowicz R.* The Barents Sea Polar Front in summer. *J. Geophys. Res*: *Oceans.* 1996, 101, C6, 14201–14221. doi: 10.1029/96jc00119
44. *Sokolov A.A.*, *Gordeeva S.M.* Change of heat advection to the Barents Sea. *Rossijskaja Arktika*. 2019, 4, 34–44 (in Russian).
45. *Timmermans M.L.*, *Labe Z.* Arctic Report Card 2020: Sea Surface Temperature, *NOAA Arctic Report Card 2020*. 2020, 1–5. doi: 10.25923/v0fs-m920
46. *Drinkwater K.F.*, *Mueter F.*, *Friedland K.D.*, *Taylor M.*, *Hunt G.L.*, *Hare J.*, *Melle W.* Recent climate forcing and physical oceanographic changes in Northern Hemisphere regions: A review and comparison of four marine ecosystems. *Progr. Oceanogr.* 2009, 81, 1–4, 10–28. doi: 10.1016/j.pocean.2009.04.003

47. *Surkova G.V.*, *Romanenko V.A.* Barents Sea: seasonal and long-term variability of energy exchange with atmospheric. *Proc Conf* "*Morja Rossii: issledovanie beregovoj i shel'fovyh zon*". *Sevastopol', 21–25 September 2020. Sevastopol*, *MGI*, *2020.* 187–188 (in Russian).

48. *Popova V.V.* Contribution of ice cover anomalies in the Barents and Kara Seas to the circulation and temperature regimes of Northern Eurasia since the mid-1990s. *Led i Sneg.* 2020, 60, 3, 409–422 (in Russian).
doi: 10.31857/S2076673420030048

49. *Rodriguez–Puebla C.*, *Encinas A.H.*, *Nieto S.*, *Garmendia J.* Spatial and temporal patterns of annual precipitation variability over the Iberian Peninsula. *Int. J. Climatol.* 1998, 18, 3, 299–316.
doi: 10.1002/(sici)1097–0088(19980315)18:3<299:: aid-joc247>3.0.co;2-l

50. *Nesterov E.S.* North Atlantic Oscillation: atmosphere and ocean. *Moscow*, *Triada LTD*, 2013. 144 p. (in Russian).

51. *Vinogradova A.A.* Seasonal and long-term variations in atmospheric circulation indices and air mass transport to the Russian Arctic. *Optika Atmosfery i Okeana.* 2014, 27, 6, 463–472. (in Russian).

52. *Ozhigin V.K.*, *Drobysheva S.S.*, *Ushakov N.G.* Internnual variability in the physical environment, zooplankton, capelin (Mllotus villosus) and North–East Arctic cod (Gadus morhua) in the Barents Sea. *ICES Mar. Sci. Symposia*. 2003, 219, 283–293.

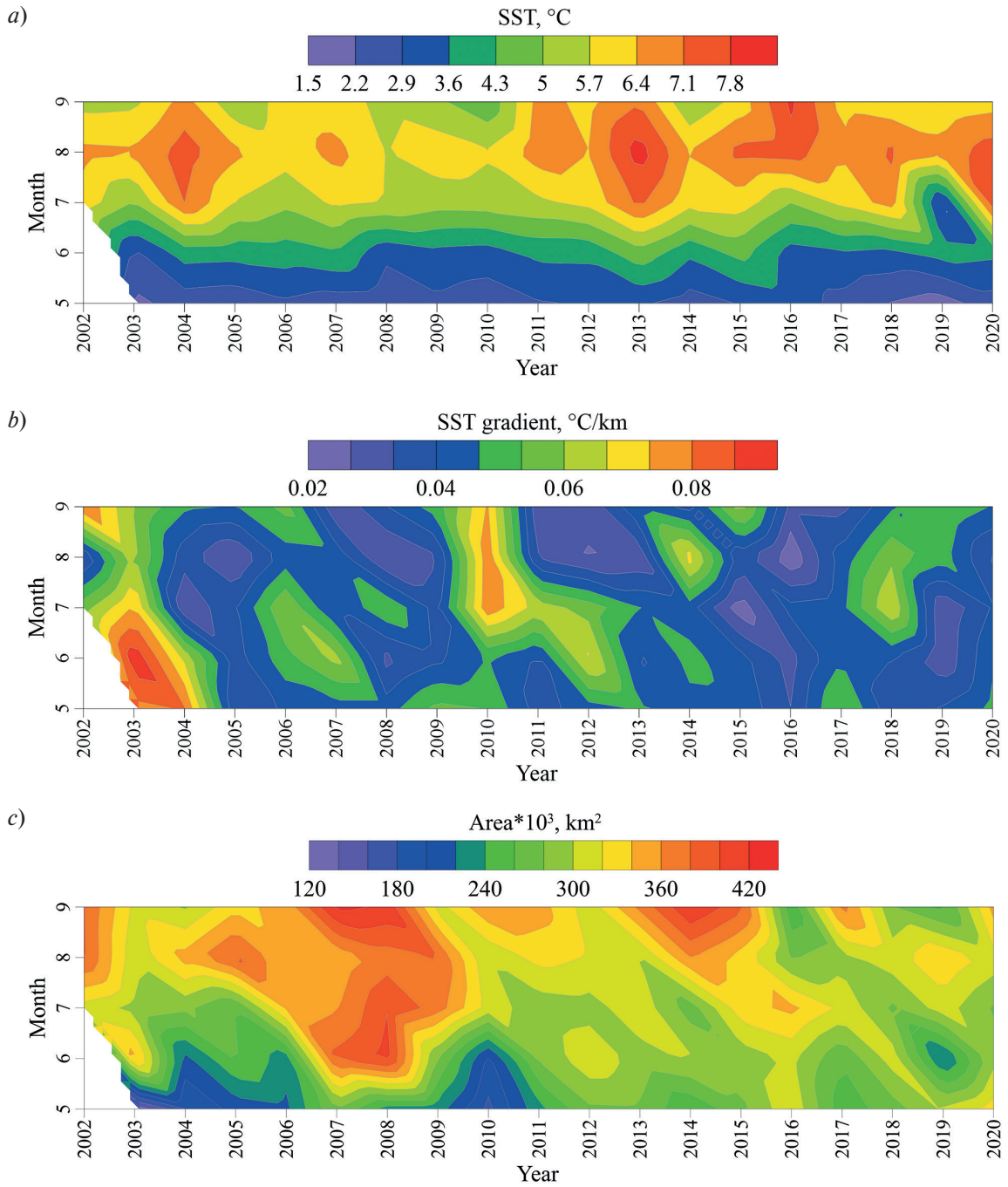

Fig. 2. Characteristic of the PFZ for the period from July 2002 to October 2020: *a* — SST; *b* — SST gradient; *c* — the area of PFZ.